Gaussian or Poisson noise?

— Comment on "A novel method for fast and robust estimation of fluorescence decay dynamics using constrained least-square deconvolution with Laguerre expansion by Liu et al., *Phys Med Biol,* 57, 843-65."

Author(s) name(s): Yongliang Zhang[1,2] and David Day-Uei Li[1]
Author Affiliation(s): [1]Centre for Biophotonics, Strathclyde Institute of Pharmacy & Biomedical Sciences, University of Strathclyde, Glasgow, Scotland, UK;
[2]College of Information Science & Electronic Engineering, Zhejiang University, Hangzhou, Zhejiang, China
E-mail: Yongliang.Zhang@strath.ac.uk; David.Li@strath.ac.uk
[*]This study was supported by the China Scholarship Council and the Royal Society.

Abstract
This comment is to clarify that Poisson noise instead of Gaussian noise shall be included to assess the performances of least-squares deconvolution with Laguerre expansion (LSD-LE) for analysing fluorescence lifetime imaging (FLIM) data obtained from time-resolved systems. Moreover, we also corrected an equation in the paper. As the LSD-LE approach is rapid and has potential to be widely applied not only for diagnostic but for wider bioimaging applications, it is desirable to have precise noise models and equations.

A – Poisson Noise Models
Liu et al. acknowledged in their paper "*no real measurement noise strictly follows an independent normal distribution. Non-normality and correlation can either be caused by limited bandwidth of detector frequency responses or be intrinsic to signal sampling schemes, such as those based on the time-correlated single-photon counting technique. Therefore, deconvolution residuals should be appropriately weighted (e.g. in case of Poisson distribution of measurement noise)*" to state that the noise do not follow normal distribution. However, instead of using Poisson noise (the dominating noise source from PMTs used in their papers or APDs), they applied Gaussian noise ("*random samples were generated with additive white Gaussian noise level ranging from 20dB to 50dB"* for comparing different deconvolution techniques and "*200 realizations fluorescence signals with 25dB additive normal noise were generated*" for selecting the Laguerre basis set) to present the signal-to-noise ratio (SNR) performances of their deconvolution methods for FLIM techniques (Liu et al., 2012). Their discussions were based on previously published papers (Jo et al., 2004) and (Pande and Jo, 2011), stating "*White noise of zero mean and three different variance levels was added to the data*" and "*Gaussian noise was added to yield two images at 40 and 25 dB SNR*" respectively. This noise model, however, does not consider the system front-ends or the Poisson noise from the PMTs(Sun et al., 2009, Sun et al., 2011). The main noise from a PMT based system is shot noise following a Poisson distribution. There is no physical way to vary the SNR once the photon count (or the acquisition time) is set (HAMAMATSU, 2016, Hall and Selinger, 1981, Li et al., 2008, Li et al., 2009). Therefore it needs to be revised, as there are no dominating factors that affect the SNR other than the acquisition time (the efficiency of detectors does not change the noise model and the Gaussian noise sources of electronics systems are usually negligible in a well-designed photon counting system). Also, using Gaussian noise will lead to an over-optimistic conclusion. Literatures and simulations will be provided to support this perspective.

Time-correlated single-photon counting (TCSPC) instruments have been the gold standard for FLIM applications (Becker, 2015, Becker, 2012). The detectors used in such systems are either photomultiplier tubes (PMT) (HAMAMATSU, 2016, Gerritsen et al., 2002) or single-photon avalanche diodes (SPAD) (Stoppa et al., 2009, Li et al., 2011, Poland et al., 2015). Usually for PMTs, there is a threshold triggering module or constant fraction discriminator to reduce the background noise before a front-end amplifier and an analogue-to-digital converter converting the signal into digital ones. For SPADs, simple latched comparators or inverters can be applied for converting a SPAD output into a digital signal compatible with the following processors. As the gains for these types of sensors are virtually infinite, the output signals generated from the front-ends become countable digital pulses (or photon events). Unlike CCD devices, they are literally readout-noise free and imperfections of electronics devices such as clock jitters or ground bounces are usually negligible.

The major noise sources for these devices are photon shot noise and dark noise (HAMAMATSU, 2016, Li et al., 2008, Li et al., 2009) manifesting themselves as photon count and dark count events in photon-counting systems, and therefore they follow a Poisson rather than a Gaussian distribution. Even for PMT devices operating in the analogue mode, the major noise does not show a Gaussian distribution (HAMAMATSU, 2016). Recent advances in semiconductor technologies have allowed these single-photon sensors to have high quantum efficiency (Webster et al., 2012) and low dark count rate (Richardson et al., 2009, Veerappan and Charbon, 2015). Nevertheless, to analyse the efficiency of a fluorescence lifetime estimation method, Poisson noise should be applied and the only way to improve the SNR is to increase the photon count (or lengthen the acquisition time). Limited improvements can be further made in terms of the efficiency of detectors, as recent developments have boosted the quantum efficiency to over 74% (Webster et al., 2012).

Simulation Results

Not knowing the exact parameters (the measured fluorescence histograms and the FWHM of the instrument impulse response function, iIRF) used in the original paper, we performed the simulations shown in Fig. 1(a) in the original paper by selecting an expected fluorescence impulse response function (fIRF) profile in MATLAB = floor(1000 exp(-t/τ)), $0 < t < 40$ns and $0.1 < \tau < 6$ns; the FWHM of the iIRF = 0.3ns; the dimension and the scale of the Laguerre basis set dimension are $L = 8$ and $0.9 < \alpha < 0.96$, respectively. For a convincing comparison with Fig. 1(a) in the original paper, the CLSD-LE and LS based lifetime estimation were applied. Poisson noise was added following the same procedures published previously (HAMAMATSU, 2016, Hall and Selinger, 1981, Li et al., 2008, Li et al., 2009). The simulations with Gaussian noise (SNR = 25dB, 40dB and 60dB, respectively) as the authors suggested were also performed for a comparison.

Figure A shows the precision and bias plots when a 40dB white Gaussian noise is added. Our simulation results follow similar trends and give similar optimised areas, $\log(\text{Bias}^2) \leq \log(\text{Variance})$, with Fig. 1(a) in the original paper suggesting that simulation procedures are similar. Figures C or D show the precision and bias plots when a 25dB or 60dB white Gaussian noise is added, respectively. On the other hand, Figure B shows the precision and bias plots when Poisson noise is added. From Figures C, A and D it seems the precision and bias can be still improved (over-optimistic) with

the SNR increased. But in fact once the photon count is fixed the noise follows Poisson distribution and the optimised area (photon counting limited) is determined.

A good indicator, F-value ($F \equiv N_C^{0.5}\sigma_\tau/\tau$, σ_τ is the standard deviation of the lifetime τ, N_C is the photon count), proposed by Gerritsen et al., 2002, can be used to check the photon efficiency of a method. Figures G, E, H and F show the F-value plots with additions of Gaussian noise (SNR = 25dB, 40dB and 60dB) and Poisson noise, respectively. Figure E shows that in the optimised area the F-value is mostly less than 1 (better than the ideal situation where F = 1), and the F-value in Fig. H is even less than 0.12, showing that the Gaussian noise model is not realistic. Figure F, on the other hand, shows that in the optimised area the F-value is indeed larger than 1 (outside the optimised area the method is bias dominated, and its F-value is less than 1, which is reasonable, see Li et al., 2011).

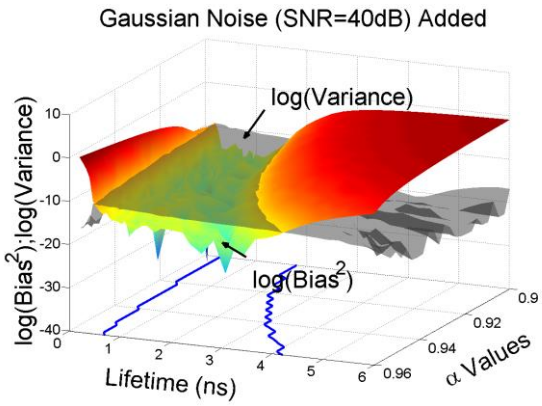

Figure A

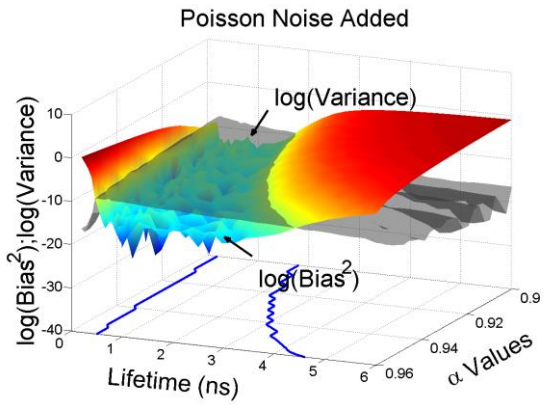

Figure B

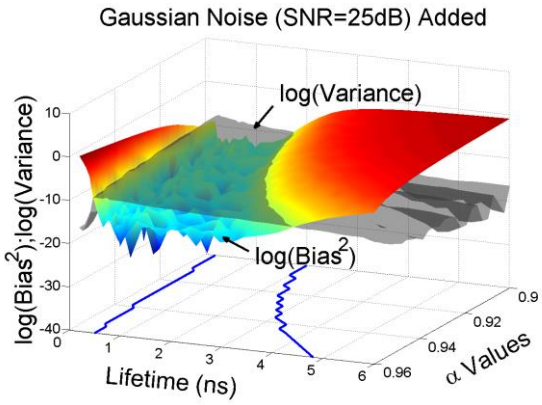

Figure C

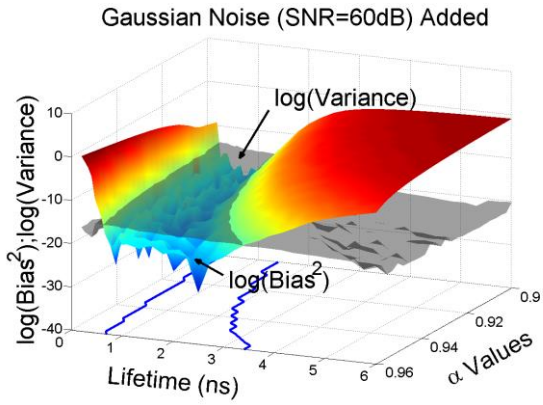

Figure D

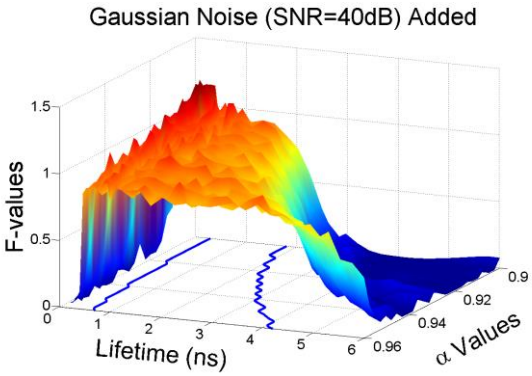

Figure E

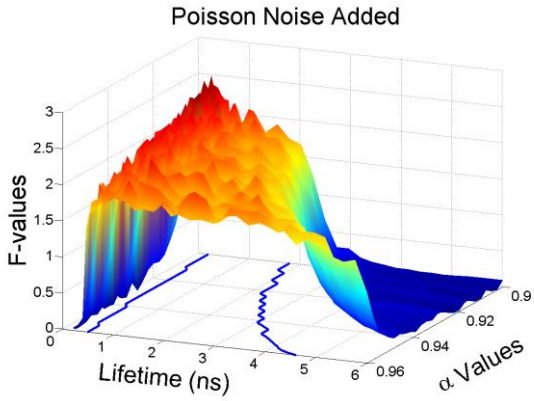

Figure F

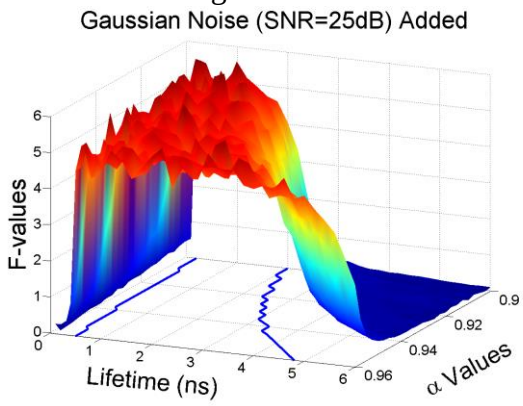

Figure G

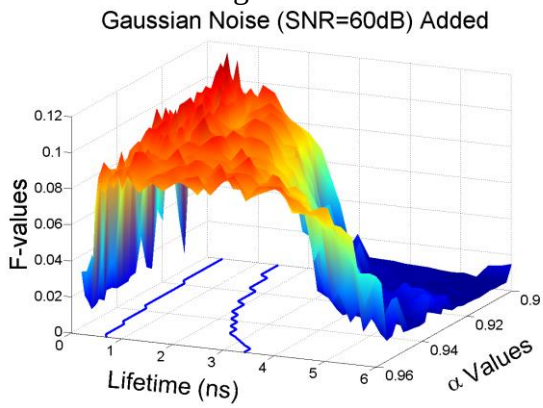

Figure H

B – The Equation to be Revised

Eq. 3 in the original paper is rewritten as

$$b_l(k;\alpha)=\alpha^{(k-l)/2}(1-\alpha)^{(1/2)}\sum_{i=0}^{l}(-1)^i\binom{k}{i}\binom{l}{i}\alpha^{l-i}(1-\alpha)^i,$$

but it causes confusion easily as the term with $k < i$ actually contributes nothing. It should be revised to

$$b_l(k;\alpha)=\alpha^{(k-l)/2}(1-\alpha)^{(1/2)}\sum_{i=0}^{l}(-1)^i\binom{k}{i}\binom{l}{i}\alpha^{l-i}(1-\alpha)^i u(k-i),$$

where $u(k)$ is a step function.

Conculsion

In this comment, we clarified that the main noise should follow a Poisson distribution instead of Gaussian distribution in a PMT based or TCSPC FLIM system by providing literatures and simulations. The simulated data with additive Poisson noise were processed to re-evaluate the LSD-LE methods presented in the original paper, and the results were compared with those using Gaussian noise suggested in the original paper. In addition, we suggested that a photon-efficiency factor *F*-value can be used to check the photon efficiency of an analysis method. With the corrected noise model and the *F*-value to link between the acquisition and the analysis accuracy, it is more straightforward for users to optimise the LSD-LE. Moreover, Eq. 3 in the original paper should be revised to avoid confusion.

References

BECKER, W. 2012. Fluorescence lifetime imaging – techniques and applications. *Journal of Microscopy,* 247**,** 119-136.

BECKER, W. 2015. The bh TCSPC Handbook, [online] Available at: http://www.becker-hickl.com/handbookphp.htm. [Accessed 23 Feb. 2016].

GERRITSEN, H. C., ASSELBERGS, M. A. H., AGRONSKAIA, A. V. & VAN SARK, W. G. J. H. M. 2002. Fluorescence lifetime imaging in scanning microscopes: acquisition speed, photon economy and lifetime resolution. *Journal of Microscopy,* 206**,** 218-224.

HALL, P. & SELINGER, B. 1981. Better estimates of exponential decay parameters. *The Journal of Physical Chemistry,* 85**,** 2941-2946.

HAMAMATSU 2016. Photomultiplier Tubes Basics and Applications, [online] Available at: https://www.hamamatsu.com/resources/pdf/etd/PMT_handbook_v3aE.pdf [Accessed 23 Feb. 2016].

JO, J. A., FANG, Q., PAPAIOANNOU, T. & MARCU, L. 2004. Fast model-free deconvolution of fluorescence decay for analysis of biological systems. *Journal of Biomedical Optics,* 9**,** 743-752.

LI, D.-U., BONNIST, E., RENSHAW, D. & HENDERSON, R. 2008. On-chip, time-correlated, fluorescence lifetime extraction algorithms and error analysis. *Journal of the Optical Society of America A,* 25**,** 1190-1198.

LI, D.-U., WALKER, R., RICHARDSON, J., RAE, B., BUTS, A., RENSHAW, D. & HENDERSON, R. 2009. Hardware implementation and calibration of background noise for an integration-based fluorescence lifetime sensing algorithm. *Journal of the Optical Society of America A,* 26**,** 804-814.

LI, D. D. U., ARLT, J., TYNDALL, D., WALKER, R., RICHARDSON, J., STOPPA, D., CHARBON, E. & HENDERSON, R. K. 2011. Video-rate fluorescence lifetime imaging camera with CMOS single-photon avalanche diode arrays and high-speed imaging algorithm. *Journal of Biomedical Optics,* 16**,** 096012-096012-12.

LIU, J., SUN, Y., QI, J. & MARCU, L. 2012. A novel method for fast and robust estimation of fluorescence decay dynamics using constrained least-squares deconvolution with Laguerre expansion. *Phys Med Biol,* 57**,** 843-65.

PANDE, P. & JO, J. A. 2011. Automated Analysis of Fluorescence Lifetime Imaging Microscopy (FLIM) Data Based on the Laguerre Deconvolution Method. *Biomedical Engineering, IEEE Transactions on,* 58**,** 172-181.

POLAND, S. P., KRSTAJI, N., MONYPENNY, J., COELHO, S., TYNDALL, D., WALKER, R. J., DEVAUGES, V., RICHARDSON, J., DUTTON, N., BARBER, P., LI, D. D.-U., SUHLING, K., NG, T., HENDERSON, R. K. & AMEER-BEG, S. M. 2015. A high speed multifocal multiphoton fluorescence lifetime imaging microscope for live-cell FRET imaging. *Biomedical Optics Express,* 6**,** 277-296.

RICHARDSON, J. A., GRANT, L. A. & HENDERSON, R. K. 2009. Low Dark Count Single-Photon Avalanche Diode Structure Compatible With Standard Nanometer Scale CMOS Technology. *Photonics Technology Letters, IEEE,* 21**,** 1020-1022.

STOPPA, D., MOSCONI, D., PANCHERI, L. & GONZO, L. 2009. Single-Photon Avalanche Diode CMOS Sensor for Time-Resolved Fluorescence Measurements. *Sensors Journal, IEEE,* 9**,** 1084-1090.

SUN, Y., PARK, J., STEPHENS, D. N., JO, J. A., SUN, L., CANNATA, J. M., SAROUFEEM, R. M. G., SHUNG, K. K. & MARCU, L. 2009. Development of a dual-modal tissue diagnostic system combining time-resolved fluorescence spectroscopy and ultrasonic backscatter microscopy. *The Review of Scientific Instruments,* 80**,** 065104.

SUN, Y., STEPHENS, D., XIE, H., PHIPPS, J., SAROUFEEM, R., SOUTHARD, J., ELSON, D. S. & MARCU, L. 2011. Dynamic tissue analysis using time- and wavelength-resolved fluorescence spectroscopy for atherosclerosis diagnosis. *Optics Express,* 19**,** 3890-3901.

VEERAPPAN, C. & CHARBON, E. 2015. A Low Dark Count p-i-n Diode Based SPAD in CMOS Technology. *Electron Devices, IEEE Transactions on,* PP**,** 1-1.

WEBSTER, E. A. G., GRANT, L. A. & HENDERSON, R. K. 2012. A High-Performance Single-Photon Avalanche Diode in 130-nm CMOS Imaging Technology. *Electron Device Letters, IEEE,* 33**,** 1589-1591.